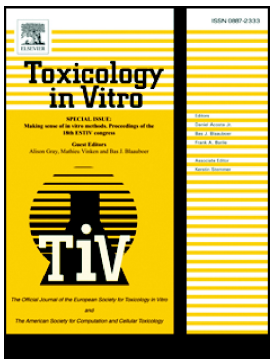

Human vasculature-on-a-chip with macrophage-mediated endothelial activation: The biological effect of aerosol from heated tobacco products on monocyte adhesion

Kazuhiro Ohashi, Ayaka Hayashida, Atsuko Nozawa, Kazushi Matsumura, Shigeaki Ito

PII: S0887-2333(23)00031-0

DOI: https://doi.org/10.1016/j.tiv.2023.105582

Reference: TIV 105582

To appear in: *Toxicology in Vitro*

Received date: 21 December 2022

Revised date: 28 February 2023

Accepted date: 13 March 2023

Please cite this article as: K. Ohashi, A. Hayashida, A. Nozawa, et al., Human vasculature-on-a-chip with macrophage-mediated endothelial activation: The biological effect of aerosol from heated tobacco products on monocyte adhesion, *Toxicology in Vitro* (2023), https://doi.org/10.1016/j.tiv.2023.105582

Title: Human vasculature-on-a-chip with macrophage-mediated endothelial activation: the biological effect of aerosol from heated tobacco products on monocyte adhesion

Authors: Kazuhiro Ohashi*, Ayaka Hayashida, Atsuko Nozawa, Kazushi Matsumura, Shigeaki Ito

Scientific Product Assessment Center, R&D Group, Japan Tobacco Inc. 6-2 Umegaoka, Aoba-ku, Yokohama 227-8512, Kanagawa, Japan

E-mail addresses: kazuhiro.ohashi@jt.com (Kazuhiro Ohashi), ayaka.hayashida@jt.com (Ayaka Hayashida), atsuko.nozawa@jt.com (Atsuko Nozawa), kazushi.matsumura@jt.com (Kazushi Matsumura), shigeaki.ito@jt.com (Shigeaki Ito)

* Correspondence should be addressed to Scientific Product Assessment Center, Japan Tobacco Inc., 6-2 Umegaoka, Aoba-ku, Yokohama, Kanagawa 227-8512, Japan. Phone: 81-80-1712-9473; E-mail: kazuhiro.ohashi@jt.com

Abstract

Heated tobacco products (HTPs) are expected to have the potential to reduce risks of smoking-associated cardiovascular disease (CVD). However, mechanism-based investigations of the effect of HTPs on atherosclerosis remain insufficient and further studies under human-relevant situations are desired for deeper understanding of the reduced risk potential of HTPs. In this study, we first developed an *in vitro* model of monocyte adhesion by considering macrophage-derived proinflammatory cytokine-mediated endothelial activation using an organ-on-a-chip (OoC), which provided great opportunities to mimic major aspects of human physiology. Then biological activities of aerosol from three different types of HTPs in terms of monocyte adhesion were compared with that of cigarette smoke (CS). Our model showed that the effective concentration ranges of tumor necrosis factor-α (TNF-α) and interleukin-1β (IL-1β) were close to the actual condition in CVD pathogenesis. The model also showed that monocyte adhesion was less induced by each HTP aerosol than CS, which may be caused by less proinflammatory cytokine secretion. In summary, our vasculature-on-a-chip model assessed the difference in biological effects between cigarettes and HTPs, and suggested a reduced risk potential of HTPs for atherosclerosis.

Keywords

Atherosclerosis, Cardiovascular disease, Organ-on-a-chip, Heated tobacco product, Monocyte adhesion, Macrophage

Abbreviations: ACM, aerosol-collected mass; CS, cigarette smoke; CVD, cardiovascular disease; DT3.0a, Direct Heating Tobacco System Platform 3 Generation 3 version a; HPHCs, harmful and potentially harmful constituents; HTP, heated tobacco product; ISO, International Organization for Standardization; MRTP, modified risk tobacco product; NP, negative control; OoC, organ-on-a-chip; PC, positive control; SE, standard error; THP, tobacco heating product; THS, tobacco heating system; TPM, total particulate matter; VC, vehicle control

1. Introduction

Atherosclerosis is the predominant cause of cardiovascular disease (CVD) that is the leading cause of death globally. In 2019, more than 30% of global deaths were estimated to be due to CVD [1]. Atherosclerosis is characterized by the formation of plaques, which disturb blood flow and eventually cause thrombosis. Several stages exist in the pathology of atherosclerosis [2] and inflammation plays major roles in all stages [3-5]. For example, proinflammatory cytokines induce endothelial dysfunction [6] that is generally found in the early stage of atherosclerosis. Zhang et al. [6] summarized the role of proinflammatory cytokines in endothelial dysfunction. Proinflammatory cytokines, such as tumor necrosis factor-α (TNF-α) and interleukin-1β (IL-1β), induce expression of adhesion molecules (e.g., intracellular adhesion molecule 1 [ICAM-1] and lectin-like oxidized low-density lipoprotein (LDL) receptor [LOX-1]). These biological events are critical for atherosclerosis development. Specifically, the expression of adhesion molecules leads to monocyte adhesion and their invasion into the intima of blood vessels [7], and LOX-1 mediates oxidized LDL uptake by macrophages [8], both of which are crucial for plaque formation. Studies have demonstrated that TNF-α [9] and IL-1β [10] deficiency reduces atherosclerotic lesions in rodent models. Although interference of innate immunity (i.e., inflammation) should be carefully considered, blockade of such proinflammatory pathways may be beneficial for atherosclerosis therapy [3]. Preventing development of a proinflammatory state is another option because various lifestyle habits, such as an unhealthy diet, low physical activity, alcohol consumption, and smoking, are known causes of systemic inflammation [11].

Smoking, which is one of the risk factors for atherosclerosis [12, 13], activates immune systems both locally and systemically [12, 14]. Cigarette smoke (CS) contains harmful and potentially harmful constituents (HPHCs) [15-17], the inhalation of which elicits various biological perturbations, including activation of circulating immune cells and tissue-resident macrophages [18]. Such immune system activation is associated with initiation and progression of atherosclerosis because immune cells are major sources of proinflammatory cytokines (e.g., TNF-α and IL-1β) [19, 20]. Therefore, reducing exposure to HPHCs may contribute to reducing the risk of atherosclerosis. Heated tobacco products (HTPs), which generate an aerosol without combustion of tobacco leaves and with fewer HPHCs in the aerosol [13, 21], are expected to achieve risk reduction associated with the smoking-related atherosclerosis risk. Zanyk et al. [22] suggested that the use of HTPs reduces the risk potential compared with conventional cigarette smoking, and Phillips et al. [23] demonstrated the potential for a reduced CVD risk of HTPs using apolipoprotein E-deficient mice. The USA FDA issued a draft guidance document for modified risk tobacco product (MRTP) application [24], and they authorized tobacco heating system (THS), especially THS 2.2, through the MRTP framework with an “exposure modification order” [25]. Therefore, further studies in human-relevant situations to understand the biological effects of HTPs on the atherosclerosis risks would provide further insights into the risk reduction potential of HTP use relative to using conventional cigarettes.

In vitro testing is a possible solution for gaining a deeper insight into the detailed mechanism in the early stage of atherosclerosis. Several *in vitro* test methods, such as the wound healing or scratch assay [26, 27] and transwell migration assay [28, 29], have been traditionally used, but the lack of physiological conditions (i.e.,

recapitulation of the effect of blood flow) may be a limitation. The emergence of microphysiological systems, also known as organ-on-a-chip (OoC), has the potential to develop more human-relevant *in vitro* models [30-32]. OoC platforms mimic the main aspects of human physiology, providing great opportunities for researchers to perform more detailed analyses including mechanistic elucidation in a reproducible and controllable manner [33]. In this study, we first developed an *in vitro* model of monocyte adhesion using OrganoPlate, a commercially available OoC. Our model includes a tubule of endothelial cells and flowing monocytes with the consideration of macrophage-mediated endothelial activation. We then examined the importance of proinflammatory cytokines for monocyte adhesion by direct treatment of endothelial tubules with TNF-α and IL-1β. The reduced risk potential of HTPs for monocyte adhesion was subsequently investigated by considering macrophage-mediated effects, assuming the actual situation of humans.

2. Materials and Methods

2.1 Cell culture

Primary human coronary artery endothelial cells (HCAECs, LOT: 425Z019.10) were purchased from PromoCell (Heidelberg, Germany) and cultured in collagen I-precoated tissue culture flasks (Corning, Corning, NY, USA) with the MV2 endothelial cell growth medium kit (PromoCell) containing a 1% penicillin-streptomycin solution (FUJIFILM Wako Pure Chemical Corporation, Osaka, Japan). Human acute monocytic leukemia cell line THP-1 (LOT: 70025047) was purchased from the American Type Culture Collection (Manassas, VA, USA) and cultured in uncoated tissue culture flasks (Corning) with Roswell Park Memorial Institute (RPMI) 1640 medium (Thermo Fisher Scientific, Waltham, MA, USA) containing 10% fetal bovine serum (FBS; Thermo Fisher Scientific, LOT: 1955174) and a 1% penicillin-streptomycin solution.

2.2 OrganoPlate culture

We used a two-lane OrganoPlate (MIMETAS, Leiden, the Netherlands) containing 96 chips with gel and perfusion channels (Fig. 1). Before seeding, 50 µL of Hank's balanced salt solution (HBSS; Thermo Fisher Scientific) was dispensed into the observation window to obtain optical clarity. Then, 2 µL of gel composed of 3 mg/mL type 1-A collagen I, which was derived from a porcine tendon, (Nitta Gelatin, Osaka, Japan, LOT: 211118, 211208), 10× minimum essential medium Hank's culture medium (Nitta Gelatin), and reconstitution buffer (Nitta Gelatin) was dispensed in the gel inlet and incubated for 15–30 minutes at 37 °C with 5% CO_2 to

complete gelation of the extracellular matrix (ECM). Each constituent was gently mixed well at ratio of 8:1:1 (v/v) to prepare 100 µL of gel in the micro tube each time. The tube was placed on ice and the mixed gel was used within 15 minutes. HCAECs at passage 3–6 were detached from flasks using 0.25% Trypsin-EDTA (Thermo Fisher Scientific) and dispensed in MV2 medium at 5×10^6 cells/mL. Next, 2 µL of cell suspension was applied to the medium inlet. After cell seeding, 50 µL of MV2 medium was added to the medium inlet. The plate was incubated on its side for 3 hours to allow the cells to attach to the ECM. Subsequently, 50 µL of MV2 medium was dispensed in the medium outlet, and the plate was placed on an MIMETAS Rocker (MIMETAS) in an incubator. The rocker was set at a 7° angle, which inverted every 8 minutes to reproduce bidirectional flow in the perfusion channel of the plate. The plate was cultured for 3–4 days until the formation of tubule structures.

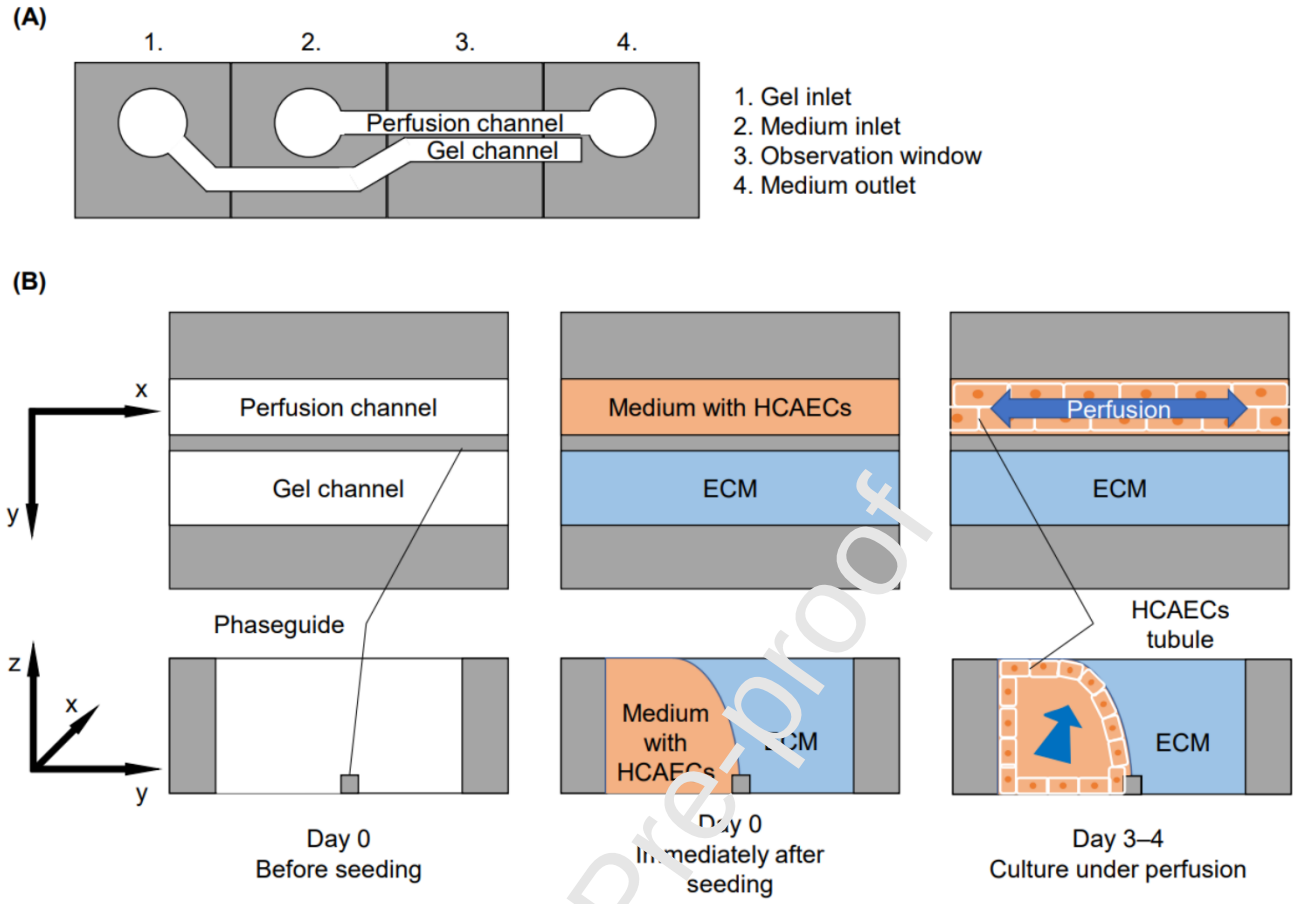

Fig. 1

Overview of the vasculature-on-a-chip model using a two-lane OrganoPlate. (A) Schematic representation of a chip on the two-lane OrganoPlate and (B) cross-section images of HCAECs tubules. Each chip consisted of two channels (i.e., perfusion and gel channels) with four wells (i.e., gel inlet, medium inlet, observation window, and medium outlet). Ninety-six chips are included in a two-lane OrganoPlate. HBSS was dispensed into the observation window to obtain optical clarity. A gel was dispensed into the gel inlet to construct an ECM and then a HCAECs suspension was applied to the medium inlet. Phaseguide consists of meticulously designed meniscus-pinning barriers that realize formation of HCAECs tubules after 3–4 days of culture under perfusion

mimicking blood flow. ECM, Extracellular matrix; HBSS, Hank's balanced salt solution; HCAECs, human coronary artery endothelial cells.

2.3 Reference conventional cigarette and HTPs

A reference conventional cigarette and three HTPs were used in this study. Kentucky reference 1R6F cigarettes were purchased from the University of Kentucky, Kentucky Tobacco Research and Development Center (Lexington, KY, USA) and stored at below 4 °C until use. Three commercial HTPs, our proprietary Direct Heating Tobacco System Platform 3 Generation 3 version a (DT3.0a), tobacco heating product (THP), and tobacco heating system (THS) with one representative regular tobacco flavor stick for each HTP were purchased from the Japanese market.

2.4 Generation of TPM and ACM solutions from cigarette and HTPs

The reference conventional cigarette and HTPs were stored for at least 48 hours at 22 ± 1 °C with 60 ± 3 % relative humidity in accordance with International Organization for Standardization (ISO) 3402 [34]. The battery of the heating device was fully charged prior to aerosol generation. Mainstream 1R6F CS and aerosols from DT3.0a, THP, and THS were generated by a RM20H smoking machine (Borgwaldt KC, Hamburg, Germany). 1R6F CS was generated under ISO 20778 (55 mL puff volume, 30 s puff interval, 2 s puff duration, bell-shaped puff profile, and 100% blocked ventilation holes) [35] and total particulate matter (TPM) was collected on a 44

mm Cambridge filter pad. Aerosol of each HTP was generated in the same manner, but without blocking the ventilation holes and aerosol-collected mass (ACM) was collected on a 44 mm Cambridge filter pad. The reason for not blocking the ventilation holes was the positions of the holes inside the device, which precluded the possibility of blocking ventilation holes under intended conditions of use. The pad was extracted with dimethyl sulfoxide (DMSO) purchased from Sigma-Aldrich (St. Louis, MO, USA) or FUJIFILM Wako Pure Chemical Corporation to prepare a 40 mg/mL TPM solution for 1R6F (accumulated from 10 sticks) and a 200 mg/mL ACM solution for DT3.0a (10 sticks), THP (12 sticks), and THS (18 sticks). The TPM and ACM solutions were stored at −80 °C until testing.

2.5 Preparation of conditioned medium from THP-1-derived macrophages

When testing, TPM and ACM solutions were diluted to 100, 200, 300, 400 µg/mL and 200, 400, 1000, 2000, 3000 µg/mL respectively by adding MV2 medium to prepare TPM and ACM samples. Each sample was 1% (TPM: 100–400 µg/mL; ACM: 200–2000 µg/mL) or 1.5% (ACM: 3000 µg/mL) adjusted with DMSO. A passage 8 THP-1 monocyte suspension was seeded in a 24-well plate (Corning) at 2×10^6 cells/well and differentiated into macrophages by stimulation with 300 nM phorbol myristate acetate (Sigma-Aldrich), 4 mM L-glutamine (FUJIFILM Wako Pure Chemical Corporation), and 500 µM monothioglycerol (FUJIFILM Wako Pure Chemical Corporation) for 48 hours and then incubated in fresh medium for 16 hours. Cells were maintained in Advanced RPMI 1640 (Thermo Fisher Scientific) containing 1% FBS and a 1% penicillin-streptomycin solution. Macrophages were exposed to 500 µL of TPM or ACM samples, MV2 medium with 1% or 1.5% DMSO, or MV2

medium with 1 μg/mL lipopolysaccharide (LPS; FUJIFILM Wako Pure Chemical Corporation) for 1 hour. After exposure, the medium was replaced with 1800 μL of MV2 medium. After 3 hours of incubation, the medium was collected and centrifuged at 1000 × *g* for 5 minutes, and the supernatant was collected as conditioned medium for each sample and stored at −80 °C until testing. An overview of conditioned medium preparation is shown in Fig. 2.

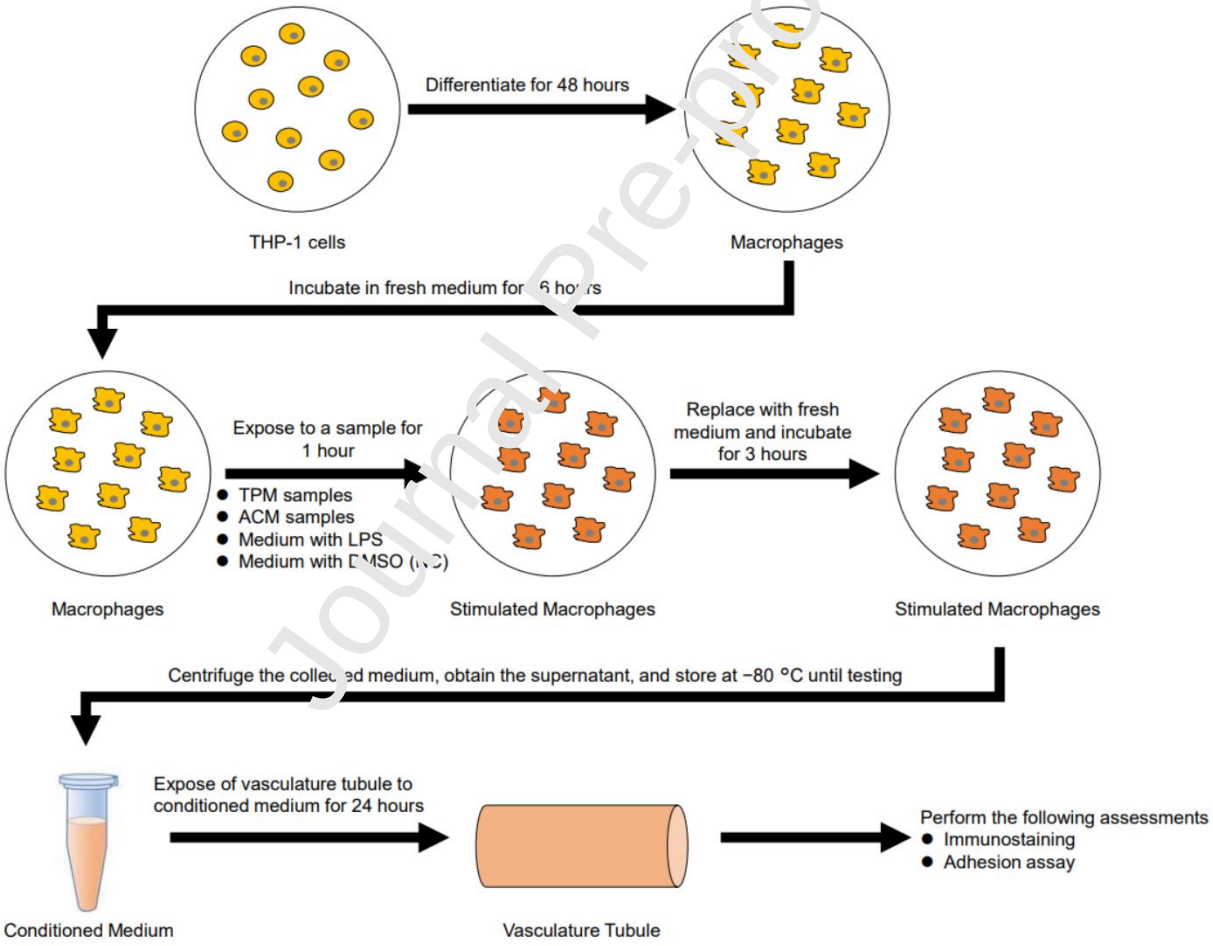

Fig. 2

Overview of the steps to prepare conditioned medium and perform immunostaining and the adhesion assay after exposure of vasculature tubules to each conditioned medium for 24 hours. ACM, aerosol-collected mass; DMSO, dimethyl sulfoxide; NC, negative control; TPM, total particulate matter.

2.6 Exposure of endothelial tubules

First, to validate monocyte adhesion assays using endothelial tubules in response to proinflammatory cytokines, endothelial tubules were exposed to several concentrations of TNF-α (Sigma-Aldrich) and IL-1β (FUJIFILM Wako Pure Chemical Corporation) test samples (12.5, 25, 50, 100, 200, 400 pg/mL respectively) and incubated on a rocker for 24 hours. MV2 medium was prepared as vehicle control (VC). Then, in another experiment, endothelial tubules were exposed to 1 µg/mL LPS-, 1R6F-, HTP-, 1% DMSO- and 1.5% DMSO-conditioned medium and incubated on a rocker for 24 hours to assess the dose response on monocyte adhesion for HTP evaluation. LPS-conditioned medium was prepared as a positive control (PC) and DMSO-conditioned medium as a negative control (NC). After exposure, immunostaining and adhesion assays were performed respectively as described in sections 2.7 and 2.8.

2.7 ICAM-1 immunostaining

After exposure, the tubules were washed with MV2 medium, fixed with a 4% paraformaldehyde phosphate buffer solution (FUJIFILM Wako Pure Chemical Corporation) for 15 minutes, and then washed twice with phosphate-buffered saline (PBS; Thermo Fisher Scientific) for 5 minutes. The cells were permeabilized with permeabilization buffer consisting of 0.3% Triton X-100 (Sigma-Aldrich) in PBS for 10 minutes. After washing with washing solution consisting of 4% FBS in PBS for 5 minutes, the cells were blocked with blocking solution

consisting of 2% FBS, 2% bovine serum albumin (Sigma-Aldrich) and 0.1% Polysorbate 20 (MP Biomedicals, Santa Ana, CA, USA) in PBS for 45 minutes. After blocking, the cells were incubated with a primary antibody solution for 90 minutes and washed twice with washing solution for 3 minutes. Next, a secondary antibody solution was applied, followed by incubation for 30 minutes. The cells were then washed twice with washing solution. Finally, MV2 medium containing Hoechst 33342 (DOJINDO) was applied, incubated for 15 minutes, and washed once with PBS. Fluorescence images were captured using an Operetta (Perkin Elmer, Waltham, MA, USA). All steps were performed at room temperature. The primary antibody used was a mouse anti-human antibody against ICAM-1 (Abcam, Cambridge, UK, LOT: GR3285740-22) diluted by blocking solution at 10 μg/mL. The secondary antibody used was goat anti-mouse Alexa Fluor 488 (Abcam, LOT: GR3419505-1) diluted by blocking solution at 2 μg/mL. Using Fiji [36] (ImageJ version 1.52e), the intensity of ICAM-1 was measured after subtraction of the background and dividing by the number of observed nuclei within each chip for quantification.

2.8 Adhesion assay

An adhesion assay was conducted to evaluate monocyte adhesion under flow. After exposure, the tubules were washed with MV2 medium and incubated with MV2 medium containing Hoechst 33342 for 20 minutes on the rocker. An undifferentiated THP-1 monocyte suspension was stained with RPMI 1640 medium containing a Calcein-AM solution (DOJINDO) for 15 minutes in the incubator. The undifferentiated THP-1 monocytes were centrifuged at 1000 × *g* for 5 minutes to remove the Calcein-AM-containing medium and resuspended in MV2

medium at 2 × 10^5 cells/mL. After washing the endothelial tubule for 5 minutes with MV2 medium, 50 µL of the undifferentiated THP-1 monocyte suspension was added to medium inlet and outlet, and incubated on the rocker for 1 hour. After washing twice with HBSS, fluorescence images were captured using the Operetta. Using Fiji, the number of undifferentiated THP-1 monocytes adhered to the endothelial surface was counted and divided by the number of endothelial cell nuclei in each chip for quantification.

2.9 WST-8 assay

To evaluate cytotoxicity, cell counting kit-8 (DOJINDO, Kumamoto, Japan) solution containing WST-8 reagent was prepared by dilution in MV2 medium before use. Macrophages prepared in the same manner described above were exposed to 500 µL of TPM or ACM sample or MV2 medium with 1% or 1.5% DMSO for 1 hour. After exposure and washing once with MV2 medium, the cell counting kit-8 solution was dispensed, followed by incubation for 2 hours. Absorbance at 450 and 600 nm was measured by a Cytation5 (BioTek Instruments, Winooski, VT, USA) before and after staining to evaluate cytotoxicity in accordance with the manufacturer's instructions.

2.10 Enzyme-linked immunosorbent assay (ELISA)

Proinflammatory cytokines TNF-α and IL-1β were measured by a Human TNF-alpha Quantikine ELISA Kit (R&D Systems, Minneapolis, MN, USA) and Human IL-1 beta/IL-1F2 Quantikine ELISA Kit (R&D Systems),

respectively, following the manufacturer's instructions. Optical density at 450 nm in each well was measured by the Cytation5. The cytokine concentration of each conditioned medium was calculated from a linear standard curve and then multiplied by the dilution factor after subtraction of the background.

2.11 Statistical analysis

The mean values and standard error (SE) for each exposure condition in each assay were calculated from replicates within the same plate and independent experiments. To normalize the difference between independent experiments, mean values of intra-experiment were first calculated. The mean values were then divided by the mean value of control from all independent experiments to calculate the fold change of each exposure condition. Statistical analysis was performed using Dunnett's multiple comparison test or Student's t-test using JMP software (version 16.2.0, SAS Institute, NC, USA). The number of replicates and independent experiments are indicated in the figure legends.

3. Results

3.1 Establishment of the monocyte adhesion assay in the vasculature-on-a-chip model with macrophages

3.1.1 Dose response of monocyte adhesion to TNF-α and IL-1β

TNF-α and IL-1β, which enhance monocyte adhesion via adhesion molecule expression on the endothelial surface, were used as PC to investigate the dose response of ICAM-1 expression and monocyte adhesion. Endothelial tubules were directly treated with PC for 24 hours. Fluorescence images of ICAM-1 expression were captured after immunostaining and their intensities were quantified to calculate the fold change (Fig. 3A). TNF-α treatment showed a dose-dependent increase of ICAM-1 expression at all examined doses. IL-1β treatment also showed a dose-dependent increase of ICAM-1 expression, which was higher than that of TNF-α treatment at all selected doses. Neither MV2 media with 1% nor 1.5% DMSO induced significant ICAM-1 expression compared with MV2 medium (vehicle control; VC). To assess monocyte adhesion, fluorescent dye-labeled monocytic THP-1 cells were applied to the tubules under flow conditions for 1 hour and then the number of THP-1 cells adhered to the endothelial surface was counted to calculate the fold change (Fig. 3B). TNF-α treatment showed a dose-dependent increase of monocyte adhesion at all examined doses. However, IL-1β treatment only showed a dose-dependent increase of monocyte adhesion at low doses (10–100 pg/mL) and reached a plateau at high doses (100–400 pg/mL). The number of adherent THP-1 cells after IL-1β treatment was more than twice as high as that after TNF-α treatment at 12.5–100 pg/mL. Neither MV2 media with 1% DMSO nor that with 1.5% DMSO induced significant monocyte adhesion compared with VC. Dose

dependency of monocyte adhesion was consistent with that of ICAM-1 expression. Representative images of ICAM-1 immunostaining and monocyte adhesion are shown in Fig. 3C and D.

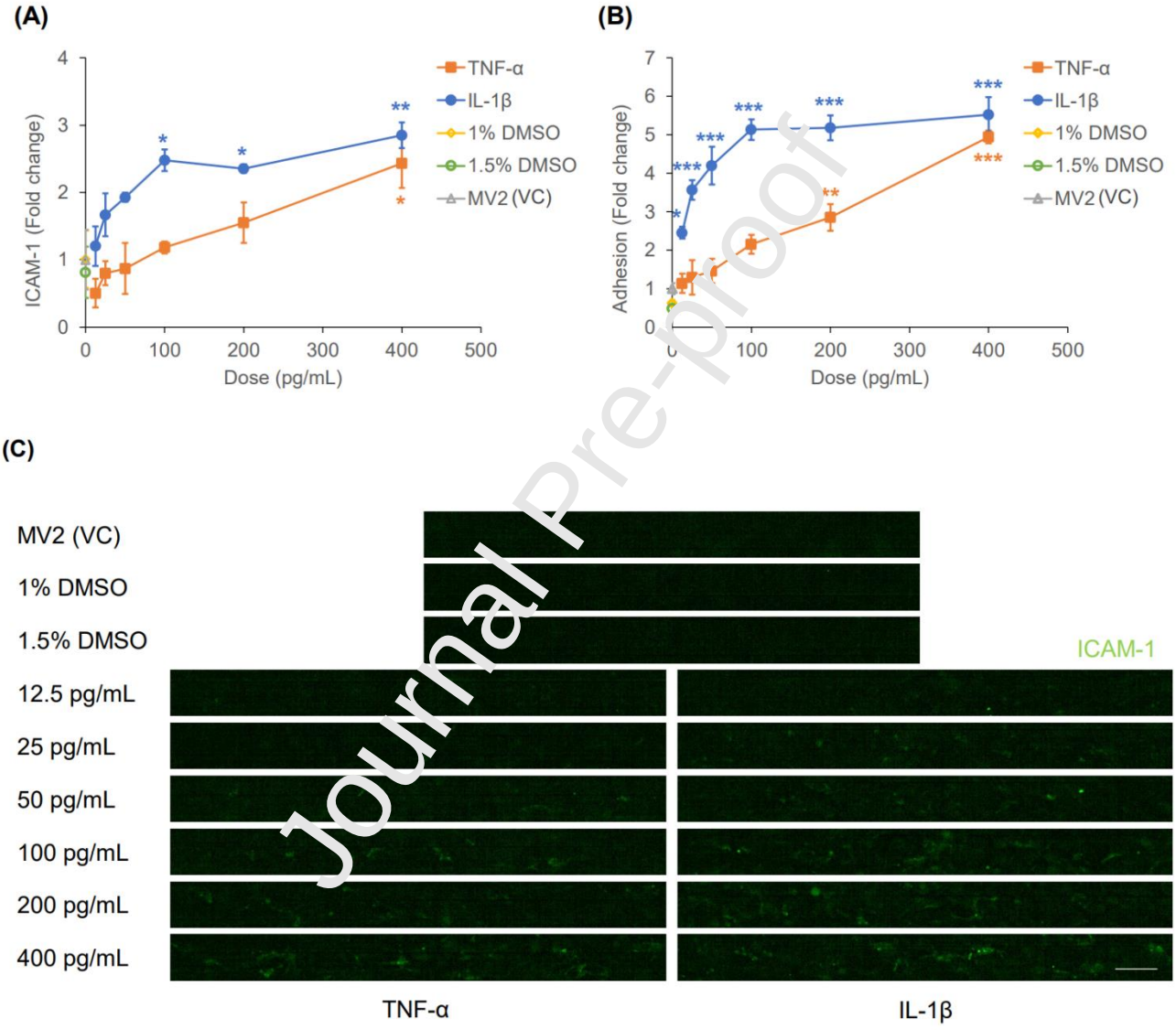

(D)

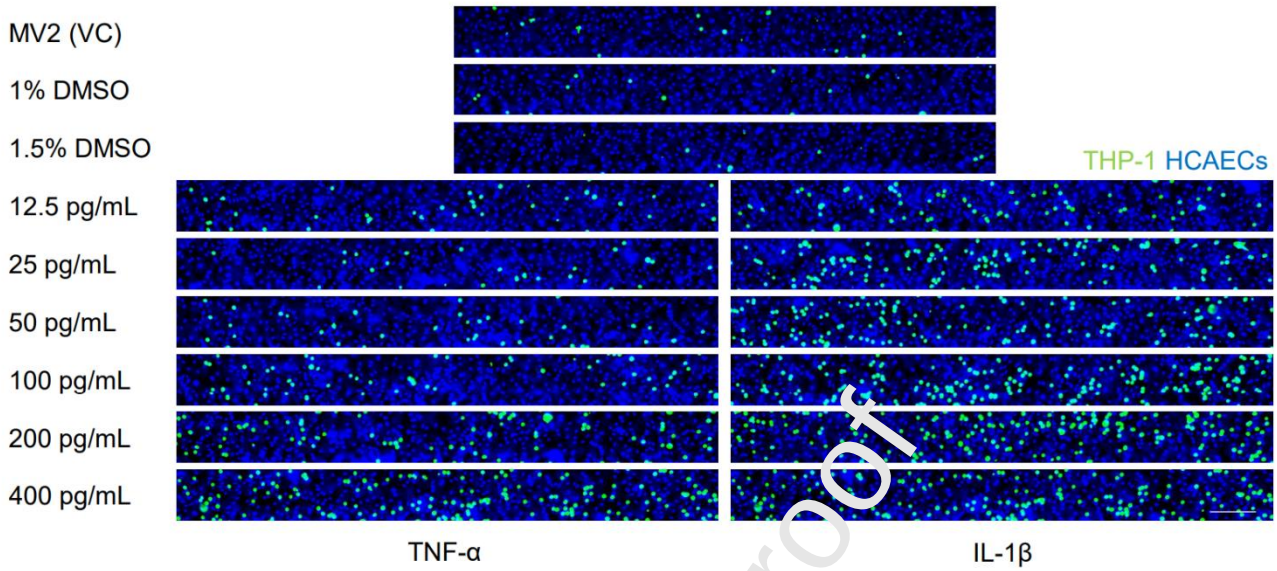

Fig. 3

Effects of proinflammatory cytokine treatment on monocyte adhesion. Dose-response curves of (A) ICAM-1 expression and (B) monocyte adhesion. (C) Fluorescence immunohistochemistry images of ICAM-1 in endothelial tubules. (D) Fluorescence images of adhered monocytes in endothelial tubules. Scale bar = 100 μm. Three individual experiments with three to four replicates in each experiment were performed. Data represent the mean ± SE of fold changes relative to VC. Asterisks indicate a statistically significant difference compared with the VC (Dunnett's multiple comparison, *p<0.05, **p<0.01, ***p<0.001). DMSO, dimethyl sulfoxide; HCAECs, human coronary artery endothelial cells; ICAM-1, intercellular adhesion molecule 1; IL-1β, interleukin-1β; MV2, endothelial cell growth medium MV2; TNF-α, tumor necrosis factor-α; VC, vehicle control.

3.1.2 Proinflammatory cytokines secreted from macrophages by LPS exposure provoke monocyte adhesion equally to TNF-α or IL-1β treatment

THP-1-derived macrophages were exposed to LPS for 1 hour and then incubated with MV2 medium for 3 hours. Cytokine-containing medium, namely conditioned medium, was obtained by centrifuging the medium and collecting the supernatant, followed by storage at −80 °C until testing. TNF-α and IL-1β concentrations quantified by the ELISAs are shown in Fig. 4A. Macrophages stimulated by LPS secreted high levels of TNF-α and IL-1β as reported previously [37]. This LPS-conditioned medium induced significant ICAM-1 expression and monocyte adhesion compared with those of MV2 medium with 1% DMSO-conditioned medium obtained without LPS stimulation (Fig. 4B). Representative images of ICAM-1 immunostaining and monocyte adhesion are shown in Fig. 4C.

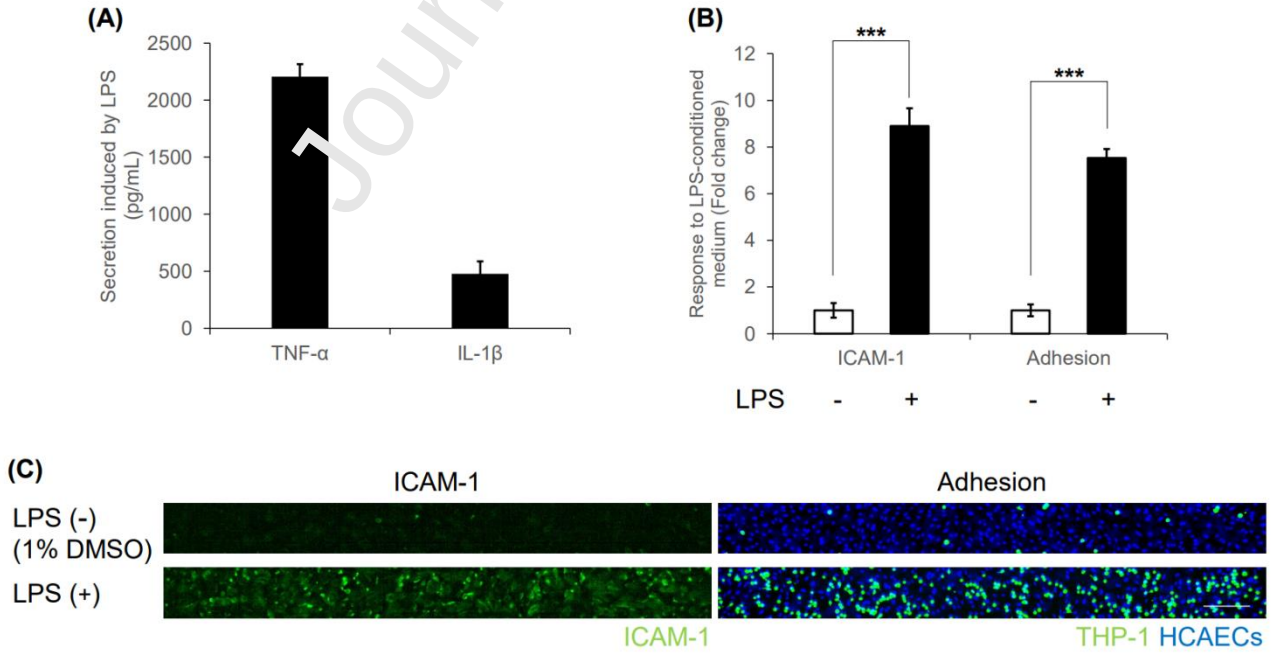

Fig. 4

Proinflammatory cytokines in LPS-conditioned medium and effect of LPS-conditioned medium exposure on monocyte adhesion. (A) Secreted TNF-α and IL-1β in LPS-conditioned medium analyzed by ELISAs, and (B) ICAM-1 expression and monocyte adhesion induced by exposure of endothelial tubules to LPS-conditioned medium. (C) Fluorescence images of ICAM-1 and adhered monocytes in endothelial tubules. Scale bar = 100 µm. Three individual experiments with three to four replicates in each experiment were performed. Data represent the mean ± SE. The fold change was relative to MV2 medium with 1% DMSO-conditioned medium obtained without LPS simulation. Asterisks indicate a statistically significant difference compared with MV2 medium with 1% DMSO-conditioned medium (Student's *t*-test, **p*<0.05, ***p*<0.01, ****p*<0.001). DMSO, dimethyl sulfoxide; ELISA, enzyme-linked immunosorbent assay; HCAECs, human coronary artery endothelial cells; ICAM-1, intercellular adhesion molecular 1; IL-1β, interleukin-1β; LPS, lipopolysaccharide; MV2: endothelial cell growth medium MV2; TNF-α, tumor necrosis factor-α.

3.2 Application of the established vasculature-on-a-chip model with macrophages to HTP evaluation

Macrophages were exposed to TPM or ACM samples or MV2 medium with DMSO (NC) to obtain each conditioned medium. Cytotoxicity in macrophages was almost the same at 1 hour of exposure to TPM or ACM samples compared with the NC in the WST-8 assay (Fig. 5A). TNF-α and IL-1β concentrations quantified by ELISAs are shown in Fig. 5B and C, respectively. The TNF-α concentration in the conditioned medium was almost the same among all conditioned media. However, 1R6F-conditioned medium showed a clear dose-dependent increase in IL-1β at 100–400 µg/mL, whose concentration was up to even four times higher than that of HTP-conditioned medium at the corresponding dose, whereas conditioned media of three HTPs did not show any significant increase compared with the NC-conditioned medium at 200–3000 µg/mL.

After exposure of endothelial tubules to the conditioned medium for 24 hours, ICAM-1 immunostaining and the adhesion assay were performed (Fig. 6A and B). The number of nuclei observed in the vessel tubules was not affected by the exposure to the conditioned medium (data not shown). 1R6F-conditioned medium induced a significantly higher increase in ICAM-1 expression in a dose-dependent manner compared with the NC-conditioned medium at 100–400 μg/mL. However, HTP-conditioned medium induced lower ICAM-1 expression compared with the 1R6F-conditioned medium at the corresponding dose and even at the higher doses. Adhesion assays showed consistent results. Monocyte adhesion was higher in the 1R6F-conditioned medium exposure compared with the HTP-conditioned medium exposure at the corresponding dose and was similar among all tested HTPs. Representative images of ICAM-1 immunostaining and monocyte adhesion are shown in Fig. 6C and D.

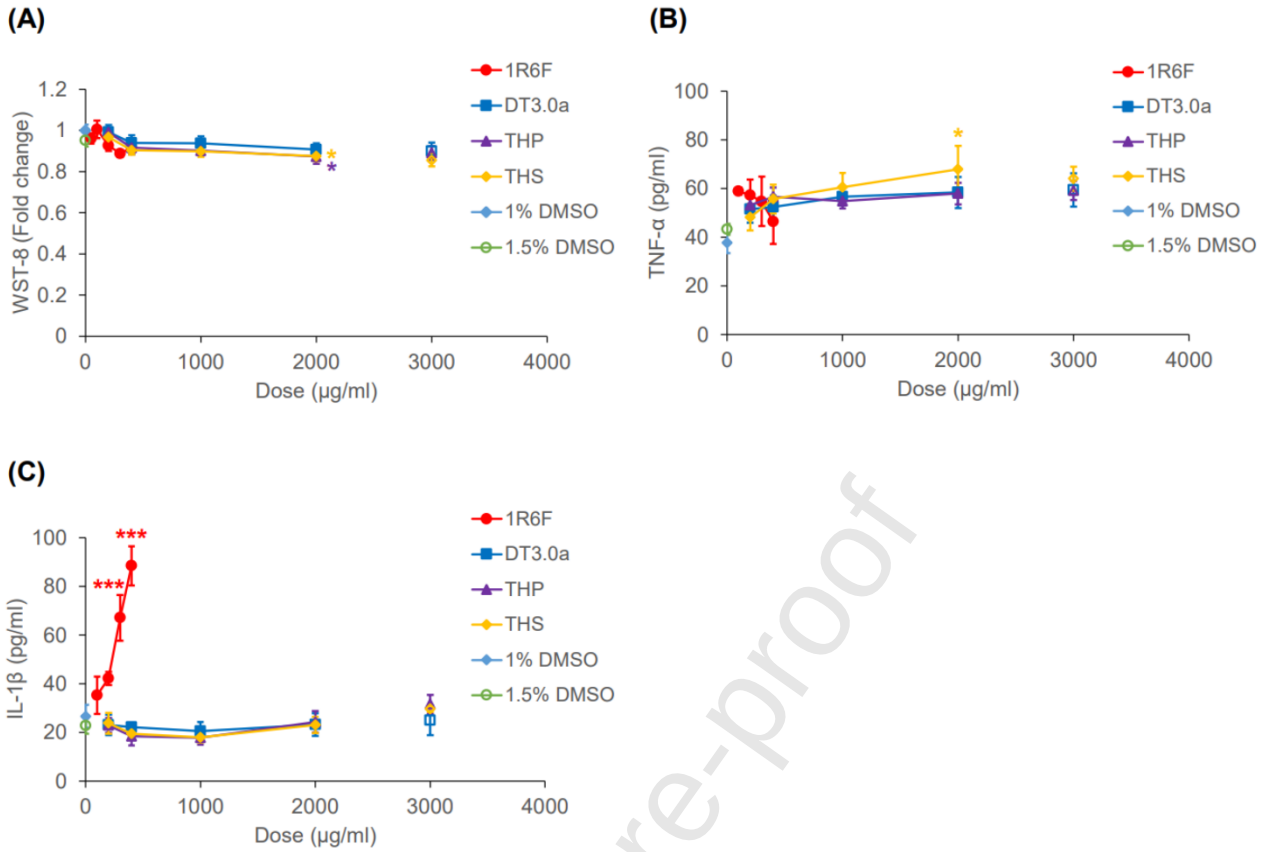

Fig. 5

Effects of 1R6F CS and HTP aerosol exposure on THP-1 derived macrophages. (A) Cytotoxicity analysis by the WST-8 assay. (B) TNF-α and (C) IL-1β in each conditioned medium analyzed by ELISAs. Three individual experiments with two to three replicates in each experiment were performed. Data represent the mean ± SE. The fold change was relative to MV2 medium with 1% DMSO-conditioned medium. Asterisks indicate a statistically significant difference compared with the NC [i.e.,1R6F: 100–400 μg/mL and HTPs: 200–2000 μg/mL were compared with MV2 medium with 1% DMSO (all filled plots) and HTPs: 3000 μg/mL were compared with MV2 medium with 1.5% DMSO (all unfilled plots)]. Dunnett's multiple comparison, *p<0.05, **p<0.01, ***p<0.001). CS, cigarette smoke; DMSO, dimethyl sulfoxide; ELISA, enzyme-linked immunosorbent

assay; HCAECs, human coronary artery endothelial cells; HTP, heated tobacco product; ICAM-1, intercellular adhesion molecular 1; IL-1β, interleukin-1β; MV2: endothelial cell growth medium MV2; SE, standard error; TNF-α, tumor necrosis factor-α.

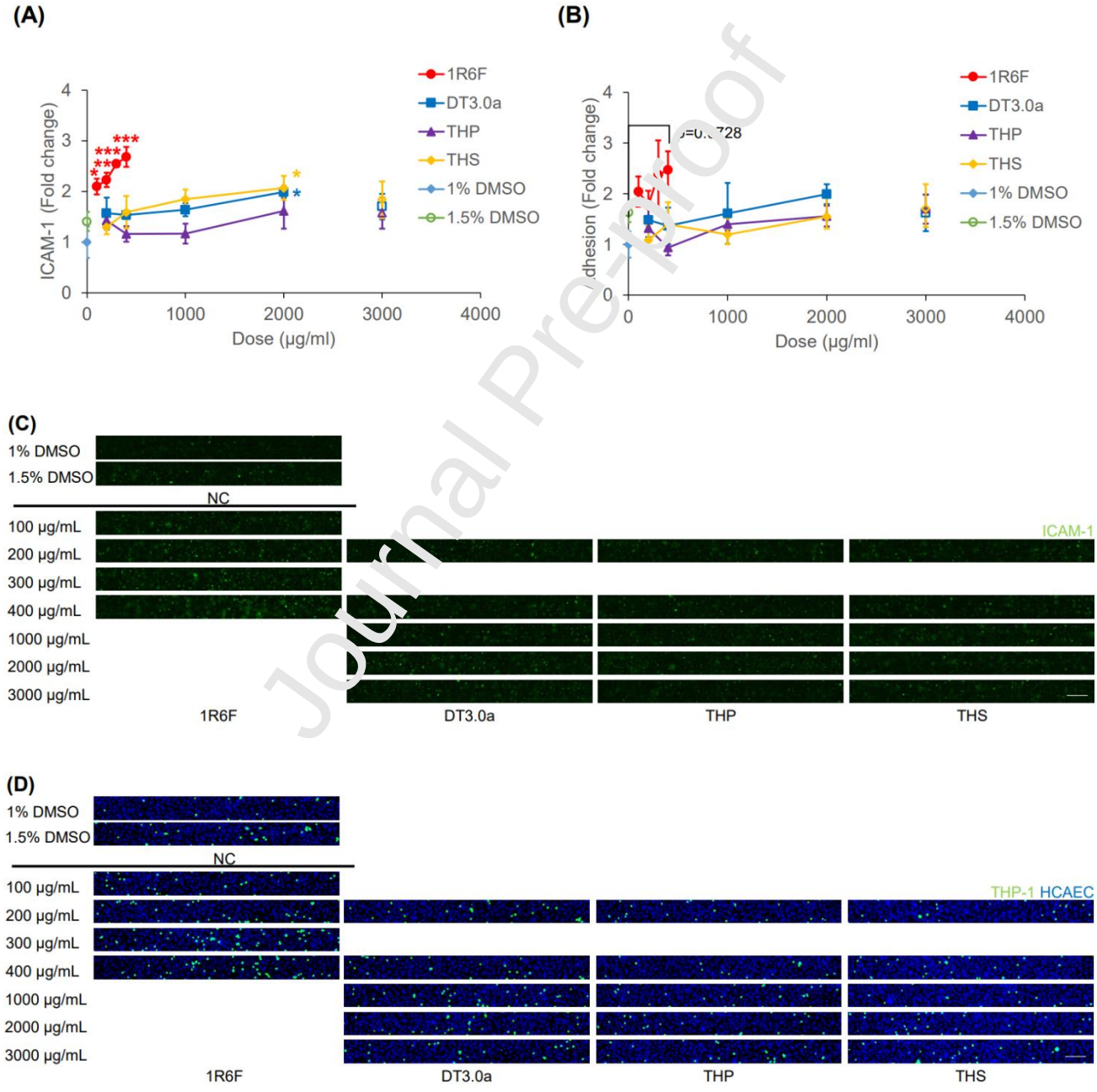

Fig. 6

Effects of 1R6F-and HTP-conditioned medium exposure on monocyte adhesion. Dose-response curves of (A) ICAM-1 expression and (B) monocyte adhesion. (C) Fluorescence immunohistochemistry images of ICAM-1 in endothelial tubules. (D) Fluorescence images of adhered monocytes in endothelial tubules. Scale bar = 100 µm. Three individual experiments with three to four replicates in each experiment were performed. Data represent the mean ± SE of fold changes relative to MV2 medium with 1% DMSO. Asterisks indicate a statistically significant difference compared with the NC [i.e.,1R6F: 100–400 µg/mL and HTPs: 200–2000 µg/mL were compared with MV2 medium with 1% DMSO (all filled plots) and HTPs: 3000 µg/mL were compared with MV2 medium with 1.5% DMSO (all unfilled plots)]. Dunnett's multiple comparison, *p<0.05, **p<0.01, ***p<0.001). CS, cigarette smoke; DMSO, dimethyl sulfoxide; ELISA, enzyme-linked immunosorbent assay; HCAECs, human coronary artery endothelial cells; HTP, heated tobacco product; ICAM-1, intercellular adhesion molecular 1; IL-1β, interleukin-1β; MV2, endothelial cell growth medium MV2; SE, standard error; TNF-α, tumor necrosis factor-α.

4 Discussion

Recent extensive studies have revealed that inflammation plays major roles in the initiation and progression of atherosclerosis. Proinflammatory cytokines, such as TNF-α and IL-1β, are mediators of vascular inflammation that induces various downstream adverse events [9, 10]. Monocyte adhesion to the vascular endothelium is one such proinflammatory cytokine-inducible event that leads to monocyte invasion into the intima, a direct cause of plaque formation [2, 7]. Therefore, we considered that evaluation of monocyte adhesion would be useful for risk estimation of HTP use for atherosclerosis. Several *in vitro* models of monocyte adhesion have been reported [38, 39], but the majority of them are established under static conditions. Considering the physiological condition of monocyte adhesion, blood flow is a critical factor in reproducing adverse events. Blood flow induces shear stress in adherent cells and may affect the extent of adhesion [40]. In this study, we developed an *in vitro* monocyte adhesion model with an OoC that recapitulates blood flow. By tilting the plate on a rocker, the model was able to generate gravity-based perfusion in the endothelial tubules, allowing cells to be exposed to shear stress up to 2.3 dyne/cm^2 [41]. Malek et al. reported that wall shear stress ranges from 10 to 70 dyne/cm^2 in normal arteries, and is relatively low (<4 dyne/cm^2) in atherosclerosis-prone arterial regions [42]. Therefore, we think that our OoC model mimics regions in coronary arteries that are susceptible to atherogenesis. Although differences of experimental conditions should be considered carefully, blood flow recapitulation might contribute to the inducibility of ICAM-1 expression and adhesion because the effective concentrations of TNF-α and IL-1β were less than 400 pg/mL in our OoC model (Fig. 3A and B), whereas the typical range was 1–10 ng/mL in previous studies [43-47]. Additionally, monocyte adhesion was obviously

increased at less than 400 pg/mL. Clinical studies have revealed that the serum level of these proinflammatory cytokines is sub-picogram to less than 100 pg/mL in CVD patients [48-50]. Therefore, the effective concentration range of proinflammatory cytokines in our OoC model mimicked the actual situation of CVD pathogenesis.

Considering the source of proinflammatory cytokines at the early stage of atherosclerosis, immune cells that mediate innate immunity could be crucial. Most tissues in the human body possess tissue-resident macrophages that play a major role in tissue-specific immune systems [51]. In the lungs, for example, when foreign harmful substances enter the lung, macrophages accumulate in the respiratory space, leading to secretion of various immune mediators [52-54]. The hypothesis that these mediators, including cytokines from the pulmonary compartment, spread via blood flow and induce systemic inflammation is supported by several studies [55-57]. To reflect the tissue-resident macrophage-mediated vascular response to cigarette or HTP exposure, we generated conditioned media. The conditioned media were generated by exposure of THP-1-derived macrophages to LPS or each extract of the cigarette or HTPs (i.e., TPM of 1R6F or ACM of each HTP). Macrophages stimulated by LPS secreted high levels of TNF-α and IL-1β as reported previously [37] and the LPS-conditioned medium induced significant ICAM-1 expression and monocyte adhesion (Fig. 4A and B), suggesting that the model reflected macrophage-mediated endothelial activation. The 1R6F-conditioned medium induced higher ICAM-1 expression and monocyte adhesion compared with all tested HTPs (Fig. 6A and B). Because TNF-α did not induce a dose-dependent increase in the conditioned medium of either 1R6F or any HTP (Fig. 5B and C), IL-1β might contribute to the increases of ICAM-1

expression and monocyte adhesion after 1R6F-conditioned medium exposure. This result is supported by proinflammatory cytokine-induced monocyte adhesion. IL-1β induced more ICAM-1 expression and monocyte adhesion than TNF-α at less than 400 pg/mL (Fig. 3). Our results suggest that IL-1β contributes more to monocyte recruitment than TNF-α at the early stage of atherosclerosis.

Our results also revealed that HTPs elicited less pronounced effects on the biological events related to monocyte adhesion even at 3000 μg/mL ACM compared with the cigarette. Furthermore, all three tested HTPs, including our DT3.0a, had comparable biological effects, although different tobacco heating mechanisms were employed. Emission of HPHCs is reduced in HTPs by heating rather than burning tobacco leaves [15, 58, 59]. Therefore, lower levels of exposure to such chemical constituents probably contribute to reducing the biological effects of HTP aerosols. The plausibility of this hypothesis has been investigated in previous studies in which traditional toxicological endpoints (e.g., cytotoxicity and genotoxicity) and effects on airway epithelial cells were evaluated, and indeed HTPs clearly exerted less pronounced effects than the cigarette [21, 60]. We believe that the results obtained in this study provide insights into the reduced risk potential of HTPs for early stage atherosclerosis.

The present study had some limitations. Although macrophages secrete various soluble mediators, we only examined TNF-α and IL-1β, which are representative proinflammatory cytokines reported to induce monocyte adhesion. In addition, considering the use of our OoC model for HTP risk assessment, the sample exposure conditions could be improved. We exposed differentiated macrophages to TPM and ACM, and thus, macrophages were not exposed to gas-vapor phase (GVP) extract. GVP derived from CS contains several

reactive oxygen species, which are thought to induce oxidative stress-mediated inflammatory responses [61]. Although Hashizume et al. indicated that GVP derived from HTPs induced negative or weak oxidative stress compared with CS [62], it would be beneficial to conduct testing using GVP samples for a better understanding of the biological effect caused by the gaseous phase of samples. In terms of the TPM and ACM sample concentrations, we used concentrations in the range 100–400 and 200–3000 μg/mL, respectively. Charles et al. estimated that active smokers had airway nicotine concentrations of 70–850 ng/mL [63]; therefore, TPM and ACM ranges in the airways could be calculated to be approximately 1.6–20.2 and 2.2–60.7 μg/mL, respectively, based on the report by Hashizume et al. [62]. Our experimental concentrations might be higher than in real-world situations; however, the results sufficiently recapitulated the mechanism of action for atherogenesis. Thus, considering the complex nature and chronicity of atherogenesis, long-term exposure similar to real-life exposure scenarios would be also valuable for additional insights into the reduced-risk potential of HTPs. This study also examined the limited stage of atherosclerosis (i.e., early stage); therefore, the later stage of atherosclerosis (e.g., transmigration of monocytes, oxidized LDL uptake, and foam cell formation by monocyte-derived macrophages) should be investigated further. The OrganoPlate platform has the potential to reproduce the later stage of atherosclerosis because of its flexibility and feasibility for *in vitro* model development. For example, other cell types, such as smooth muscle cells, can be applied to be more physiologically relevant. Such an improved model may be useful for further mechanistic understanding and risk estimation of atherosclerosis.

5 Conclusion

OoC-based *in vitro* test systems are expected to recapitulate the physiological conditions in the human body. Here, we first developed an *in vitro* model of monocyte adhesion using a vasculature-on-a-chip platform, which also mimicked tissue-resident macrophage-mediated endothelial activation. The model showed that the effective concentration range of TNF-α and IL-1β was close to the actual situation in CVD pathogenesis. The model also showed that monocyte adhesion was induced less by HTP aerosols than by CS, which may be caused by less proinflammatory cytokine secretion from macrophages. Although further studies are necessary, our OoC model detects differences in the biological effects of a cigarette and HTPs, and a reduced risk potential of HTPs for atherosclerosis was suggested.

Declaration of Competing Interest

This work was funded by Japan Tobacco Inc., and all authors are employees of this company.

Acknowledgments

The authors are grateful to Dr. Takashi Sekine, Dr. Yuichi Furudono and Dr. Hitoshi Fujimoto for their supports in conducting this study. The authors are grateful to Dr. Tsuneo Hashizume for his advice on writing this article. We also thank Mitchell Arico and J. Ludovic Croxford, PhD, from Edanz (https://jp.edanz.com/ac) for editing a draft of this manuscript.

Funding Information

Japan Tobacco Inc. was the sole source of funding for this project. No external sources of funding were used for this project.

References

1. WHO, Cardiovascular diseases (CVDs), (2021).
2. Rader, D.J. and A. Daugherty, *Translating molecular discoveries into new therapies for atherosclerosis.* Nature, 2008. **451**(7181): p. 904-13.
3. Libby, P., *Interleukin-1 Beta as a Target for Atherosclerosis Therapy: Biological Basis of CANTOS and Beyond.* J Am Coll Cardiol, 2017. **70**(18): p. 2278-2289.
4. Pearson, T.A., et al., *Markers of inflammation and cardiovascular disease: application to clinical and public health practice: A statement for healthcare professionals from the Centers for Disease Control and Prevention and the American Heart Association.* Circulation, 2003. **107**(3): p. 499-511.
5. Chen, J., et al., *Recent Progress in in vitro Models for Atherosclerosis Studies.* Front Cardiovasc Med, 2021. **8**: p. 790529.
6. Zhang, H., et al., *Role of TNF-alpha in vascular dysfunction.* Clin Sci (Lond), 2009. **116**(3): p. 219-30.
7. Libby, P., P.M. Ridker, and G.K. Hansson, *Progress and challenges in translating the biology of atherosclerosis.* Nature, 2011. **473**(7347): p. 317-25.
8. Pirillo, A., G.D. Norata, and A.L. Catapano, *LOX-1, OxLDL, and atherosclerosis.* Mediators Inflamm, 2013. **2013**: p. 152786.
9. Branen, L., et al., *Inhibition of tumor necrosis factor-alpha reduces atherosclerosis in apolipoprotein E knockout mice.* Arterioscler Thromb Vasc Biol, 2004. **24**(11): p. 2137-42.
10. Kirii, H., et al., *Lack of interleukin-1beta decreases the severity of atherosclerosis in ApoE-deficient mice.* Arterioscler Thromb Vasc Biol, 2003. **23**(4): p. 656-60.
11. Furman, D., et al., *Chronic inflammation in the etiology of disease across the life span.* Nat Med, 2019. **25**(12): p. 1822-1832.
12. Messner, B. and D. Bernhard, *Smoking and cardiovascular disease: mechanisms of endothelial dysfunction and early atherogenesis.* Arterioscler Thromb Vasc Biol, 2014. **34**(3): p. 509-15.
13. Ambrose, J.A. and R.S. Barua, *The pathophysiology of cigarette smoking and cardiovascular disease: an update.* J Am Coll Cardiol, 2004. **43**(10): p. 1731-7.
14. Shiels, M.S., et al., *Cigarette smoking and variations in systemic immune and inflammation markers.* J Natl Cancer Inst, 2014. **106**(11).
15. Forster, M., et al., *Assessment of novel tobacco heating product THP1.0. Part 3: Comprehensive chemical characterisation of harmful and potentially harmful aerosol emissions.* Regul Toxicol Pharmacol, 2018. **93**: p. 14-33.
16. Margham, J., et al., *Chemical Composition of Aerosol from an E-Cigarette: A Quantitative Comparison with Cigarette Smoke.* Chem Res Toxicol, 2016. **29**(10): p. 1662-1678.
17. Tayyarah, R. and G.A. Long, *Comparison of select analytes in aerosol from e-cigarettes with smoke from conventional cigarettes and with ambient air.* Regul Toxicol Pharmacol, 2014. **70**(3): p. 704-10.
18. Lugg, S.T., et al., *Cigarette smoke exposure and alveolar macrophages: mechanisms for lung disease.* Thorax, 2022. **77**(1): p. 94-101.

19. Hansson, G.K. and A. Hermansson, *The immune system in atherosclerosis.* Nat Immunol, 2011. **12**(3): p. 204-12.
20. Wolf, D. and K. Ley, *Immunity and Inflammation in Atherosclerosis.* Circ Res, 2019. **124**(2): p. 315-327.
21. Schaller, J.P., et al., *Evaluation of the Tobacco Heating System 2.2. Part 2: Chemical composition, genotoxicity, cytotoxicity, and physical properties of the aerosol.* Regul Toxicol Pharmacol, 2016. **81 Suppl 2**: p. S27-S47.
22. Znyk, M., J. Jurewicz, and D. Kaleta, *Exposure to Heated Tobacco Products and Adverse Health Effects, a Systematic Review.* Int J Environ Res Public Health, 2021. **18**(12).
23. Phillips, B., et al., *An 8-Month Systems Toxicology Inhalation/Cessation Study in Apoe-/- Mice to Investigate Cardiovascular and Respiratory Exposure Effects of a Candidate Modified Risk Tobacco Product, THS 2.2, Compared With Conventional Cigarettes.* Toxicol Sci, 2016. **149**(2): p. 411-32.
24. FDA, Modified Risk Tobacco Product Applications, (2012).
25. FDA, Modified Risk Orders. IQOS System Holder and Charger, (2020).
26. Taylor, M., et al., *A comparative assessment of e-cigarette aerosols and cigarette smoke on in vitro endothelial cell migration.* Toxicol Lett, 2017. **277**: p. 123-128.
27. Fearon, I.M., D.O. Acheampong, and E. Bishop, *Modification of smoke toxicant yields alters the effects of cigarette smoke extracts on endothelial migration: an in vitro study using a cardiovascular disease model.* Int J Toxicol, 2012. **31**(6): p. 572-83.
28. van der Toorn, M., et al., *Aerosol from a candidate modified risk tobacco product has reduced effects on chemotaxis and transendothelial migration compared to combustion of conventional cigarettes.* Food Chem Toxicol, 2015. **86**: p. 81-7.
29. van der Toorn, M., et al., *A prototypic modified risk tobacco product exhibits reduced effects on chemotaxis and transendothelial migration of monocytes compared with a reference cigarette.* Food Chem Toxicol, 2015. **80**: p. 274-286.
30. Kim, S., et al., *Vasculature-On-A-Chip for In Vitro Disease Models.* Bioengineering (Basel), 2017. **4**(1).
31. Poussin, C., et al., *3D human microvessel-on-a-chip model for studying monocyte-to-endothelium adhesion under flow - application in systems toxicology.* ALTEX, 2020. **37**(1): p. 47-63.
32. Makwana, O., et al., *Impact of cigarette versus electronic cigarette aerosol conditioned media on aortic endothelial cells in a microfluidic cardiovascular model.* Sci Rep, 2021. **11**(1): p. 4747.
33. Leung, C.M., et al., *A guide to the organ-on-a-chip.* Nature Reviews Methods Primers, 2022. **2**(1).
34. ISO, Tobacco and tobacco products — Atmosphere for conditioning and testing, (1999).
35. ISO, ISO 20778: 2018 Cigarettes -Routine analytical cigarette smoking machine - Definitions and standard conditions with an intense smoking regime, (2018).
36. Schindelin, J., et al., *Fiji: an open-source platform for biological-image analysis.* Nat Methods, 2012. **9**(7): p. 676-82.
37. Lopez-Bojorquez, L.N., et al., *NF-kappaB translocation and endothelial cell activation is potentiated by macrophage-released signals co-secreted with TNF-alpha and IL-1beta.* Inflamm Res, 2004. **53**(10): p. 567-75.

38. Poussin, C., et al., *In vitro systems toxicology-based assessment of the potential modified risk tobacco product CHTP 1.2 for vascular inflammation- and cytotoxicity-associated mechanisms promoting adhesion of monocytic cells to human coronary arterial endothelial cells.* Food Chem Toxicol, 2018. **120**: p. 390-406.
39. Rajesh, M., et al., *CB2-receptor stimulation attenuates TNF-alpha-induced human endothelial cell activation, transendothelial migration of monocytes, and monocyte-endothelial adhesion.* Am J Physiol Heart Circ Physiol, 2007. **293**(4): p. H2210-8.
40. Chiu, J.J., S. Usami, and S. Chien, *Vascular endothelial responses to altered shear stress: pathologic implications for atherosclerosis.* Ann Med, 2009. **41**(1): p. 19-28.
41. Vriend, J., et al., *Flow stimulates drug transport in a human kidney proximal tubule-on-a-chip independent of primary cilia.* Biochim Biophys Acta Gen Subj, 2020. **1864**(1): p. 129433.
42. Malek, A., et al., Hemodynamic shear stress and its role in atherosclerosis, Jama, 282(21), 2035-2042.
43. Chen, P.J., et al., *Honokiol suppresses TNF-alpha-induced neutrophil adhesion on cerebral endothelial cells by disrupting polyubiquitination and degradation of IkappaBalpha.* Sci Rep, 2016. **6**: p. 26554.
44. Meliton, A.Y., et al., *Phosphodiesterase 4 inhibition of beta2-integrin adhesion caused by leukotriene B4 and TNF-alpha in human neutrophils.* Eur Respir J, 2006. **28**(5): p. 920-8.
45. Azcutia, V., et al., *Inflammation determines the pro-adhesive properties of high extracellular d-glucose in human endothelial cells in vitro and rat microvessels in vivo.* PLoS One, 2010. **5**(4): p. e10091.
46. Cheng, S.C., et al., *Quercetin Inhibits the Production of IL-1beta-Induced Inflammatory Cytokines and Chemokines in ARPE-19 Cells via the MAPK and NF-kappaB Signaling Pathways.* Int J Mol Sci, 2019. **20**(12).
47. Zhao, W., et al., *Danshenol A inhibits TNF-alpha-induced expression of intercellular adhesion molecule-1 (ICAM-1) mediated by NOX4 in endothelial cells.* Sci Rep, 2017. **7**(1): p. 12953.
48. Xing, J., Y. Liu, and T. Chen, *Correlations of chemokine CXCL16 and TNF-alpha with coronary atherosclerotic heart disease.* Exp Ther Med, 2018. **15**(1): p. 773-776.
49. Di Iorio, A., et al., *Serum IL-1β levels in health and disease: a population-based study. 'The InCHIANTI study'.* Cytokine, 2003. **22**(6): p. 198-205.
50. Monteiro, A.M., et al., *Cardiovascular disease parameters in periodontitis.* J Periodontol, 2009. **80**(3): p. 378-88.
51. Davies, L.C., et al., *Tissue-resident macrophages.* Nat Immunol, 2013. **14**(10): p. 986-95.
52. Hogg, J.C., *Pathophysiology of airflow limitation in chronic obstructive pulmonary disease.* The Lancet, 2004. **364**(9435): p. 709-721.
53. Vlahos, R. and S. Bozinovski, *Role of alveolar macrophages in chronic obstructive pulmonary disease.* Front Immunol, 2014. **5**: p. 435.
54. Yamasaki, K. and S.F.V. Eeden, *Lung Macrophage Phenotypes and Functional Responses: Role in the Pathogenesis of COPD.* Int J Mol Sci, 2018. **19**(2).
55. Sinden, N.J. and R.A. Stockley, *Systemic inflammation and comorbidity in COPD: a result of 'overspill' of inflammatory mediators from the lungs? Review of the evidence.* Thorax, 2010. **65**(10): p. 930-6.

56. Tamagawa, E., et al., *Particulate matter exposure induces persistent lung inflammation and endothelial dysfunction.* Am J Physiol Lung Cell Mol Physiol, 2008. **295**(1): p. L79-85.
57. Nurkiewicz, T.R., et al., *Systemic microvascular dysfunction and inflammation after pulmonary particulate matter exposure.* Environ Health Perspect, 2006. **114**(3): p. 412-9.
58. Schaller, J.P., et al., *Evaluation of the Tobacco Heating System 2.2. Part 3: Influence of the tobacco blend on the formation of harmful and potentially harmful constituents of the Tobacco Heating System 2.2 aerosol.* Regul Toxicol Pharmacol, 2016. **81 Suppl 2**: p. S48-S58.
59. Hirn, C., et al., *Comparative and cumulative quantitative risk assessments on a novel heated tobacco product versus the 3R4F reference cigarette.* Toxicol Rep, 2020. **7**: p. 1502-1513.
60. Thorne, D., et al., *Assessment of novel tobacco heating product THP1.0. Part 7: Comparative in vitro toxicological evaluation.* Regul Toxicol Pharmacol, 2018. **93**: p. 73-83.
61. Sekine, T., C. Sakaguchi, and Y. Fukano, *Investigation by microarray analysis of effects of cigarette design characteristics on gene expression in human lung mucoepidermoid cancer cells NCI-H292 exposed to cigarette smoke.* Exp Toxicol Pathol, 2015. **67**(2): p. 143-51.
62. Hashizume, T., et al., *Chemical and in vitro toxicological comparison of emissions from a heated tobacco product and the 1R6F reference cigarette.* Toxicology Reports, 2023.
63. Esther, C.R., Jr., et al., *Prolonged, physiologically relevant nicotine concentrations in the airways of smokers.* Am J Physiol Lung Cell Mol Physiol, 2023. **324**(1): p. L32-L37.

Declaration of interests

☐ The authors declare that they have no known competing financial interests or personal relationships that could have appeared to influence the work reported in this paper.

☒The authors declare the following financial interests/personal relationships which may be considered as potential competing interests:

This work was funded by Japan Tobacco Inc., and all authors are employees of this company.

Highlights

- *In vitro* model of monocyte adhesion was developed using OoC.
- Inflammatory cytokine-mediated endothelial activation by macrophages was reflected.
- Effective doses of TNF-α and IL-1β were close to CVD pathogenesis.
- Monocyte adhesion was less induced by HTPs than by cigarette.